Schlieren Imaging of Ultrasound Wave Interference

Faith Poutoa,[a)] Adrian Rodriguez, Len Welstand, Mary Becker, Miche Maral, Sydnie Duckworth, Ryan Palmares, Chris Patino, and Matthew E. Anderson

Department of Physics, San Diego State University, Planetarium Court, San Diego, California 92182, USA

[a)]Corresponding author: fpoutoa0822@sdsu.edu

Abstract. This study uses schlieren photography to visualize the interference patterns of ultrasonic sound waves in air. By capturing variations in a region's refractive index, direct, real-time images of wave interactions are produced. Our system enhances the understanding of acoustic phenomena and demonstrates the feasibility of low-cost schlieren setups for educational and research applications.

INTRODUCTION

Schlieren photography offers a powerful method for capturing images of transparent phenomena, including sound waves, which are otherwise invisible to the human eye. Sound waves are longitudinal, mechanical waves that propagate through a medium by creating alternating regions of high and low pressure. These pressure variations alter the medium's density, resulting in subtle changes to its refractive index n. By translating these variations into visible brightness contrasts, schlieren photography is well suited for studying acoustic disturbances with remarkable clarity, as it highlights phase disturbances in transparent media. August Toepler originally applied Foucault's knife-edge test to visualize acoustic waves in 1864. Since then, schlieren photography has undergone significant advancements that merit further exploration in sound wave visualization.[1] The term "schlieren," derived from the German word for "streaks," describes the technique's ability to reveal fluid flow patterns such as streaks and swirls.

While other methods like shadowgraphy[2] also capitalize on variations in refractive index to visualize fluid or wave disturbances, these approaches lack the sensitivity of schlieren imaging for capturing acoustic waves. Shadowgraphy relies on higher-order changes in the index of refraction, making it less effective for visualizing detailed ultrasonic wave propagation.[3] This study presents a replicable and cost-effective schlieren photography setup tailored for imaging ultrasonic waves and other physical phenomena. In addition to acoustic wave visualization, our setup demonstrates airflow patterns, making it an invaluable tool for physics education. Its affordability and ease of use make it suitable for demonstrations at both K–12 and undergraduate levels, enriching the learning experience with accessible and fascinating visualizations of complex physical principles.

THEORY

In elementary optics, Snell's law is used to describe the manner in which light travels through different media at different speeds and thus bends at an angle dependent on the ratio of the refractive indices of the two media. However, schlieren imaging is a result of the bending of light, or refraction, as it passes through a region of varying refractive index within the same transparent medium. Simply put, light rays bend toward regions of higher index. The theoretical discussion that follows is adapted from Settles.[1]

The refractive index and density of air are related by the Gladstone-Dale law,[4] and when combined with the ideal gas law yield

$$n - 1 = k\rho = \frac{kP}{RT}, \tag{1}$$

where n is the index of refraction, ρ is the density of air, k is the molar refractivity, P is the pressure, R is the ideal gas constant, and T is the temperature.

Equation (1) tells us that the index of refraction of a medium is proportional to pressure. Acoustic sound waves, whether they are traveling or standing waves, create regions of alternating high and low pressure. For a sinusoidal ultrasonic sound wave traveling in the y direction and sampled at $t = 0$, we can write

$$P = P_0 \sin\left(\frac{2\pi y}{\lambda}\right), \tag{2}$$

and substituting into Eq. (1), we find the index as a function of y,

$$n(y) - 1 = \frac{k}{RT} P_0 \sin\left(\frac{2\pi y}{\lambda}\right). \tag{3}$$

Schlieren imaging is sensitive to angular ray deflection, which is proportional to the gradient of the index of refraction. This is shown in Fig. 1. Following Settles,[1] it can be shown that the ray deflection angle ε is given by

$$\varepsilon = \frac{L}{n_0}\frac{\partial n}{\partial y} = \left(\frac{2\pi k}{n_0 RT}\right)\left(\frac{LP_0}{\lambda}\right)\cos\left(\frac{2\pi y}{\lambda}\right), \tag{4}$$

where L is the interaction length, which is the distance along the axis of propagation for the light beam, and n_0 is the refractive index of the surrounding medium in the absence of sound waves.[1]

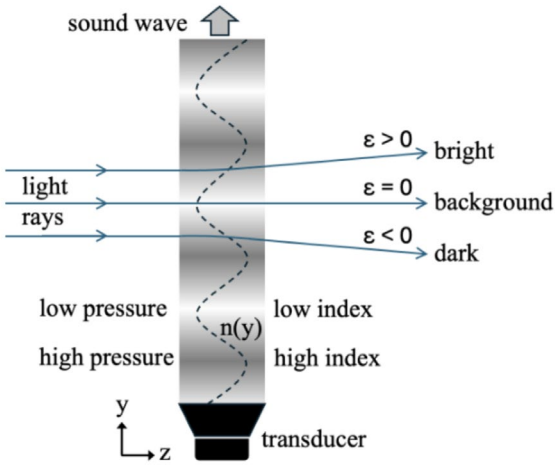

FIGURE 1. Diagram of light rays interacting with an ultrasound wave.

Since schlieren imaging projects 3D fluid disturbances onto a 2D image, one can evaluate the intensity of changes happening in the test space by evaluating their luminance intensity relative to the background. Contrast C refers to the level of changing luminance relative to its background and is given by[1]

$$C = \frac{f}{a}\,\varepsilon = \left(\frac{2\pi k}{n_0 RT}\right)\left(\frac{fLP_0}{a\lambda}\right)\cos\left(\frac{2\pi y}{\lambda}\right), \tag{5}$$

where f is the focal length and a is the portion of the light source image that is not blocked by the razor blade. Notice that since the expression for ε has a factor of $\cos\left(\frac{2\pi y}{\lambda}\right)$, it may be positive or negative. When $\varepsilon < 0$, the razor blade in our experimental schlieren setup blocks the downward-deflected light, creating dark spots in positions of negative gradients in pressure. Similarly, if $\varepsilon > 0$, then our setup will produce bright spots in locations with positive gradients in pressure. Referring back to Eq. (5), the second term contains experimental variables we can optimize: focal length f, interaction length L, and sound pressure P_0. A long-focal-length mirror, a deeper sound field, and a stronger sound wave, respectively, are preferable for our purposes. Additionally, contrast is inversely proportional to the wavelength λ of the sound wave; thus high-frequency ultrasound is easier to detect. It is also relevant to note that due to the differentiation of $n(y)$ within the given equation for angular wave deflection, there is a 90° phase shift between the functions that describe the acoustic behavior of the sound wave and the schlieren contrast image.

EXPERIMENT OVERVIEW

As shown in Fig. 2, a pulsed LED shines through a pinhole and expands to uniformly illuminate a 12-inch parabolic mirror of focal length 1.2 meters that was removed from a telescope (Sky-Watcher Quattro 300P). The region adjacent to the mirror, referred to as the "test area," contains the disturbances under investigation. The light is refocused back

to a focal spot where a razor blade is positioned to partially obstruct the light. Both the pinhole and the razor blade are roughly 2*f* from the mirror. The unblocked portion of the light is then captured by a video camera, which records the schlieren image for analysis. The partial obstruction of focused light by the razor blade increases the contrast between regions with varying refractive indices, allowing slight variations in the light beam's path to be translated into differences in brightness. Areas where the light is bent to a greater extent will be displayed as either darker or lighter, depending on the direction of the deviation. For alignment, we found it important to be able to translate the razor blade precisely on an XYZ translator, and likewise to orient it appropriately. For vertically traveling sound waves, a horizontal razor orientation is necessary because the sound waves will deflect light rays vertically, thereby highlighting the sound waves' structure.

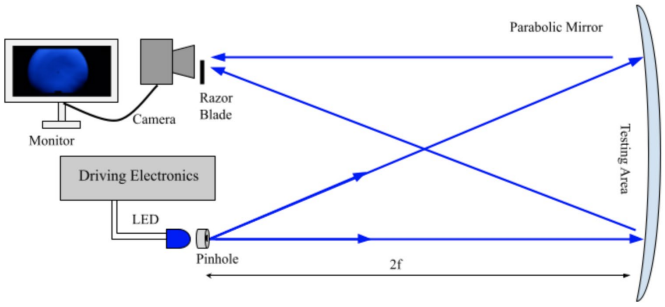

FIGURE 2. Schematic diagram of the schlieren optical system used in the experiment.

Pulsed LED and Transducers

An LED is strobed to the sound waves emitted by an ultrasonic transducer (HiLetgo, TCT40-16R/T, 10W). Strobing the LED's pulses to specific points in the sound wave's cycle allows for a clear capture of the wave's structure while also highlighting details in pressure differences. Both the LED and transducer are driven by an arbitrary function generator (UNI-Trend, UTG932E) connected to an amplifier (Nobsound, NS-03G FR). These particular transducers are designed to function primarily at 40.3 kHz (we found a very narrow linewidth around this resonant frequency). With this high frequency, the ultrasound wave's density variations are closely spaced, making them easier for the schlieren system to detect than longer audible wavelengths. In this particular experiment, we found good contrast with a blue LED, but relevant papers have been successful in using different colors to capture sound wave images.[4]

Sound Wave Interference

A notable phenomenon associated with sound waves is interference. To visualize this effect, two ultrasonic transducers were employed, both operating in-phase at a frequency of 40.3 kHz and positioned adjacent to each other. The direct schlieren image illustrating this interference is presented in Fig. 3(a), which shows a central maximum and first-order interference on either side. To enhance the contrast of the image, we utilized ImageJ (imagej.net) to subtract the background with the ultrasound off and subsequently adjust the brightness and contrast mapping functions. The resulting enhanced image is displayed in Fig. 3(b).

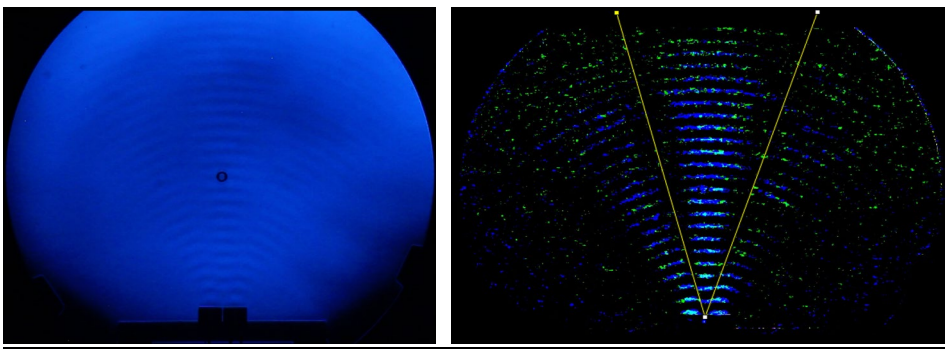

(a) (b)

FIGURE 3. (a) Direct schlieren image of sound wave interference and (b) the filtered image. Note: In (a) the center spot is an alignment guide for the primary mirror.

The image reveals a characteristic two-slit interference pattern, which occurs as the sound waves combine constructively and destructively. For further analysis, ImageJ enables direct measurements within the image. Initially, we scaled the pixel dimensions using known quantities, such as the physical size of the transducers. This allowed us to measure various parameters, including the separation between the speakers, the individual wavelengths, and the angle between the maxima or minima, as indicated by the yellow lines in Fig. 3(b). The diffraction equation for two-slit interference is given by $d\sin\theta = m\lambda$, where d is the separation of the transducers, θ is the angle from central maximum, m is the order (integer for maxima, half-integer for minima), and λ is the wavelength. As seen in Fig. 2(b), we identify the locations of the minima. Using $m = \pm 1/2$, $d = 17$ mm, and the full angle $2\theta = 30° \pm 2°$, we calculate a wavelength $\lambda = 8.8 \pm 0.5$ mm. This is in good agreement (within 4%) with the theoretical wavelength calculated from the speed of sound, λ = (343 m/s)/(40.3 kHz) = 8.5 mm, or by direct measurement of the calibrated image, which indicated $\lambda = 8.6$ mm.

CONCLUSION

This project demonstrates schlieren imaging of ultrasonic sound waves. Setup and execution require minimal maintenance, making this experiment well suited for lecture and laboratory demonstrations. It should also be noted that while ultrasound does not fall into the audible range, ear protection should be worn at all times during the experiment. Future work on this project lies in imaging increasingly complex fields of acoustic interference while also investigating developments in acoustic holography. By utilizing the pressure differences created by acoustic interference, small objects can be levitated within the nodes of a standing wave. We plan to modify the open-source software Ultraino, along with its associated hardware driver boards that control the ultrasonic phased array.[5] The end goal is to levitate multiple particles whose movement can be controlled by user input in the Ultraino software. Interested readers can refer to the references for a discussion of the theory behind acoustic holography and ultrasonic levitation.[6,7]

ACKNOWLEDGMENTS

The authors would like to thank Dr. David Pullman, Dr. Fletcher Miller, and Dr. Jan Chaloupka for technical advice during this project. This work was generously supported by a Society of Physics Students Chapter Research Award.

REFERENCES

1. G. S. Settles, *Schlieren and Shadowgraph Techniques: Visualizing Phenomena in Transparent Media* (Springer, Berlin, New York, 2001), pp. 2–11, 25–50, 338–340.
2. G. S. Settles and M. J. Hargather, "A review of recent developments in schlieren and shadowgraph techniques," Meas. Sci. Technol. **28**(4), 042001 (2017).
3. G. S. Settles, E. B. Hackett, L. M. Weinstein, and J. D. Miller, Full-scale schlieren flow visualization, in *Flow Visualization II*, *Proceedings of the Intl. Symposium on Flow Visualization*, edited by J. P. Crowder (Begell House, Danbury, CT, 1995), pp. 2–13.
4. A. Crockett and W. Rueckner, "Visualizing sound waves with schlieren optics," Am. J. Phys. **86**(11), 870–876 (2018).
5. A. Marzo, T. Corkett, and B. W. Drinkwater, "Ultraino: An open phased-array system for narrowband airborne ultrasound transmission," IEEE Trans. Ultrason. Ferroelectr. Freq. Control **65**(1), 102–111 (2018).
6. R. Hirayama, G. Christopoulos, D. Martinez Plasencia, and S. Subramanian, "High-speed acoustic holography with arbitrary scattering objects," Sci. Adv. **8**(24), eabn7614 (2022).
7. Y. Ochiai, T. Hoshi, and J. Rekimoto, "Three-dimensional mid-air acoustic manipulation by ultrasonic phased arrays," PLoS One **9**(5), e97590 (2014).